⌘ *Author's Choice*

THE JOURNAL OF BIOLOGICAL CHEMISTRY VOL. 283, NO. 28, pp. 19301–19313, July 11, 2008

Structural Determinants of Ca^{2+} Permeability and Conduction in the Human 5-Hydroxytryptamine Type 3A Receptor*[S]

Received for publication, March 27, 2008, and in revised form, May 8, 2008 Published, JBC Papers in Press, May 12, 2008, DOI 10.1074/jbc.M802406200

Matthew R. Livesey[‡1], Michelle A. Cooper[‡], Tarek Z. Deeb[§], Jane E. Carland[‡], Janna Kozuska[‡], Tim. G. Hales[§¶], Jeremy J. Lambert[‡2], and John A. Peters[‡2,3]

From the [‡]Neurosciences Institute, Division of Pathology and Neuroscience, Ninewells Hospital and Medical School, University of Dundee, Dundee DD1 9SY, Scotland, United Kingdom and the [§]Departments of Pharmacology and Physiology and [¶]Anesthesiology and Critical Care Medicine, George Washington University, Washington, D. C. 20037

Cation-selective cysteine (Cys)-loop transmitter-gated ion channels provide an important pathway for Ca^{2+} entry into neurones. We examined the influence on Ca^{2+} permeation of amino acids located at intra- and extracellular ends of the conduction pathway of the human 5-hydroxytryptamine type 3A (5-HT_{3A}) receptor. Mutation of cytoplasmic arginine residues 432, 436, and 440 to glutamine, aspartate, and alanine (the aligned residues of the human 5-HT_{3B} subunit (yielding 5-HT_{3A}(QDA)) increased P_{Ca}/P_{Cs} from 1.4 to 3.7. The effect was attributable to the removal of an electrostatic influence of the Arg-436 residue. Despite its relatively high permeability to Ca^{2+}, the single channel conductance of the 5-HT_{3A}(QDA) receptor was depressed in a concentration-dependent and voltage-independent manner by extracellular Ca^{2+}. A conserved aspartate, located toward the extracellular end of the conduction pathway and known to influence ionic selectivity, contributed to the inhibitory effect of Ca^{2+} on macroscopic currents mediated by 5-HT_{3A} receptors. We introduced a D293A mutation into the 5-HT_{3A}(QDA) receptor (yielding the 5-HT_{3A}(QDA D293A) construct) to determine whether the aspartate is required for the suppression of single channel conductance by Ca^{2+}. The D293A mutation decreased the P_{Ca}/P_{Cs} ratio to 0.25 and reduced inwardly directed single channel conductance from 41 to 30 pS but did not prevent suppression of single channel conductance by Ca^{2+}. The D293A mutation also reduced P_{Ca}/P_{Cs} when engineered into the wild-type 5-HT_{3A} receptor. The data helped to identify key residues in the cytoplasmic domain (Arg-436) and extracellular vestibule (Asp-293) that markedly influence P_{Ca}/P_{Cs} and additionally directly demonstrated a depression of single channel conductance by Ca^{2+}.

The 5-hydroxytryptamine type 3 (5-HT_3)[4] receptor is a cation-selective ligand-gated ion channel of the Cys-loop superfamily with structural and functional homology to the family of nicotinic acetylcholine (ACh) receptors (1–3). 5-HT_3 receptor activation elicits rapidly activating and desensitizing inward current responses mediated by the flux of both mono- and divalent cations (2). 5-HT_3 receptor stimulation contributes to fast excitatory synaptic transmission in the central nervous system (4–7) and also modulates the release of several neurotransmitters including acetylcholine, cholecystokinin, dopamine, glutamate, norepinephrine, and particularly γ-aminobutyric acid, the exocytosis of which is enhanced by direct Ca^{2+} influx through the ionophore of presynaptic 5-HT_3 receptors (8, 9).

5-HT_3 receptors can be assembled *in vitro* as pentamers from a selection of five gene products, namely the 5-HT_{3A}, 5-HT_{3B}, 5-HT_{3C}, 5-HT_{3D}, and 5-HT_{3E} subunits (10–16). The 5-HT_{3A} subunit assembles as a functional homopentamer and is mandatory for cell surface expression of any of the other 5-HT_3 receptor subunits (10, 14, 17). Only homopentameric 5-HT_{3A} and heteropentameric 5-HT_{3A}/5-HT_{3B} subunit complexes have been characterized in detail (10–12). These two receptor types differ in their sensitivity to activation by 5-HT, antagonism by certain agents, and allosteric modulation by some general anesthetics and 5-substituted indole analogues (11, 12, 18, 19). Strikingly, the human homomeric 5-HT_{3A} receptor exhibits an unusually small single channel conductance within the range of 0.3 to 1 pS (20–22), whereas the corresponding range of 16 to 30 pS for the human 5-HT_{3A}/5-HT_{3B} heteromer (11, 23) is more akin to the single channel conductance of most native 5-HT_3 receptors and other members of the Cys-loop receptor superfamily family. Heteromeric 5-HT_{3A}/5-HT_{3B} receptors additionally differ from the homomeric 5-HT_{3A} isoform by exhibiting a reduced relative permeability to Ca^{2+}, no measurable permeability to Mg^{2+}, faster agonist-induced desensitization kinetics, and a propensity to spontaneous channel opening (11, 12, 18). Diversity within the human 5-HT_{3A} and 5-HT_{3B} subunit structure occurs through alternative splicing and polymorphisms, some of which impact significantly

* This work was supported in part by grants from the Wellcome Trust (to J. J. L. and J. A. P.), from Tenovus Scotland and the Anonymous Trust (to J. A. P.), and from the National Science Foundation (to T. G. H.). The costs of publication of this article were defrayed in part by the payment of page charges. This article must therefore be hereby marked "*advertisement*" in accordance with 18 U.S.C. Section 1734 solely to indicate this fact.

⌘ *Author's Choice*—Final version full access.

[S] The on-line version of this article (available at http://www.jbc.org) contains supplemental Fig. 1.

[1] Supported by a Biotechnology and Biological Sciences Research Council-Case studentship in conjunction with Eli Lilly and Co.

[2] Supported by a grant from Eli Lilly and Co.

[3] To whom correspondence should be addressed: Neurosciences Inst., Division of Pathology and Neuroscience, Ninewells Hospital and Medical School, The University of Dundee, Dundee DD19SY, Scotland, United Kingdom. Tel.: 44-1382-660111; Fax: 44-1382-667120; E-mail: j.a.peters@dundee.ac.uk.

[4] The abbreviations used are: 5-HT, 5-hydroxytryptamine; ACh, acetylcholine; MA, membrane-associated; TM, transmembrane; pS, picosiemens; HEK, human embryonic kidney; *I-V*, whole-cell current-voltage relationship; *i-V*, single channel current-voltage relationship.

upon receptor expression and function and are linked to human pathologies (23–25).

Cys-loop receptor subunits share a common overall topology of extracellular, transmembrane (TM), and intracellular domains, which represent functionally interacting modules (26, 27) (Fig. 1*A*). The TM domain consists of four α-helices (TM1–4), the second of which (TM2) lines the ion channel (26, 27). A wealth of evidence across both cation- and anion-selective channels of the Cys-loop family implicate specific amino acid residues within TM2 and the adjacent sequences as fundamental determinants of ionic selectivity and single channel conductance (2, 26, 28–30) (Fig. 1*B*).

Notwithstanding the importance of the TM2 domain, we have identified an additional α-helical structure (the MA helix) within the large intracellular loop linking TM3 and TM4 that greatly influences single channel conductance (2, 22, 31, 32) (Fig. 1*C*). In particular, the peculiarly small single channel conductance of the human homomeric 5-HT_{3A} receptor is due to the unique presence of three arginine residues (Arg-432, Arg-436, and Arg-440) that impede cation conductance by both steric and repulsive electrostatic influences (32). The combined substitution of these residues by those aligned in the human 5-HT_{3B} receptor subunit (*i.e.* R432Q, R436D, R440A, generating a construct coined 5-HT_{3A}(QDA)) enhances single channel conductance by ~40-fold (22, 33) (Fig. 1*C*). Importantly, arginine residues engineered into the corresponding locations of both subunit species of the nicotinic ACh $\alpha_4\beta_2$ receptor depress single channel conductance (22). Such findings have been rationalized in the light of the 4 Å resolution model of the nicotinic ACh receptor of *Torpedo marmorata* in which the five MA-stretch helices manifest as an inverted pentagonal cone that projects from the plasma membrane into the cytoplasm forming the intracellular vestibule of the channel (26). Narrow (~8 Å) lateral windows (or "portals") situated at the subunit interfaces, which are lined by the MA helices, form an obligate pathway for ion permeation (26) (Fig. 1*A*).

Here, we demonstrate that residues within the MA helices also strongly affect the permeability of Ca^{2+} relative to monovalent ions (*e.g.* P_{Ca}/P_{Cs}) but do not influence charge selectivity (*e.g.* P_{Na}/P_{Cl}). Additionally, we describe the influence of Ca^{2+} on 5-HT-evoked single channel conductance using the 5-HT_{3A}(QDA) construct as a model, which, unlike the wild-type receptor, mediates unitary events that can be directly resolved in outside-out patch recordings. Finally, we have examined the role of an aspartate residue, located at the extracellular end of the conduction pathway, which is known to influence ionic conductance and selectivity in other Cys-loop receptors (28) and contributes to an inhibitory effect of Ca^{2+} on macroscopic currents mediated by 5-HT_{3A} receptors (34). The introduction of a D293A mutation into the 5-HT_{3A}(QDA) receptor (yielding the 5-HT_{3A}(QDA D293A) construct) markedly suppressed P_{Ca}/P_{Cs} and reduced inwardly directed single channel conductance.

EXPERIMENTAL PROCEDURES

5-HT_{3A} Receptor Constructs and Transfection of cDNAs—cDNAs encoding human wild-type and mutant 5-HT_{3A} receptor subunits were cloned into pGW1 (17). Point mutations were introduced using standard molecular biological techniques (31), and all cDNAs were sequenced to confirm fidelity. Wild-type and mutant receptor subunit cDNAs were co-transfected into tsA-201 or HEK-293 cells, with a cDNA encoding green fluorescent protein to identify transfected cells. Transfection was performed by electroporation (400 V, 125 microfarads, infinite resistance) using a Bio-Rad Gene Electropulser II (Bio-Rad) or the calcium phosphate precipitation method. Transfected cells were routinely cultured in Dulbecco's modified Eagle's medium supplemented with 10% (v/v) fetal bovine serum, 2 mM glutamine, 1 mM sodium pyruvate, 100 μg ml^{-1} streptomycin, and 100 units ml^{-1} penicillin and maintained at 37 °C for 24–48 h in 95% air, 5% CO_2 at 100% humidity before use.

Electrophysiological Recordings—Whole-cell and outside-out patch configurations were used to record macroscopic and single channel currents, respectively, from transfected cells. All experiments were performed at room temperature (20–23 °C). The recording chamber was routinely superfused (5 ml min^{-1}) with an extracellular solution (E1) comprising (in mM): NaCl 140, KCl 2.8, $MgCl_2$ 2.0, $CaCl_2$ 1.0, glucose 10, HEPES 10 (pH 7.2, adjusted with 1 M NaOH; final $[Na^+]_o$ = 146 mM). Patch electrodes (resistance = 2–8 megohms when measured in solution E1) were filled with an intracellular solution (I1) containing (in mM): CsCl 140, $CaCl_2$ 0.1, EGTA 1.1, HEPES 10 (pH 7.2, adjusted by 1 M CsOH, final $[Cs^+]_i$ = 143 mM). In solution I2, CsCl was totally replaced by NaCl (pH 7.2, adjusted by 1 M NaOH, final $[Na^+]_i$ = 145 mM). The intracellular free calcium concentration ($[Ca^{2+}]_i$) for I1 and I2 was estimated to be 10 nM (35). To determine the relative permeability of Na^+ *versus* Cs^+ (P_{Na}/P_{Cs}), in solution E2, additional NaCl totally replaced KCl in the extracellular solution, and the concentrations of $CaCl_2$ and $MgCl_2$ were each reduced to 0.1 mM to minimize the influence of divalent cations upon the reversal potential of the macroscopic current response to 5-HT ($E_{5\text{-}HT}$). The permeability of Ca^{2+} relative to Cs^+ (P_{Ca}/P_{Cs}) was determined using an extracellular solution (E3) containing (in mM): $CaCl_2$ 100, L-histidine 5, glucose 10 (pH 7.2) (20). To prevent changes in reference electrode potential during the superfusion of media with altered ionic composition, a bridge containing 3 M KCl in agar (4% w/v) was employed. Liquid junction potentials arising at the tip of the patch pipette were measured as described by Fenwick *et al.* (35), and potential measurements were corrected post hoc.

$E_{5\text{-}HT}$ was determined by two methods. In the first, the membrane potential was stepped from −60 mV to −100 mV for 100 ms and subsequently ramped to +60 mV within 1 s at the peak of the macroscopic current response to pressure-applied 5-HT (1 μM). Care was taken to ensure that the agonist-induced current recorded at −60 mV before and immediately following the voltage ramp did not change. Subtraction of the leakage current recorded in the absence of 5-HT from the current recorded in the presence of the agonist yielded the current-voltage (*I-V*) relationship attributable to the 5-HT-evoked conductance increase. In the second method, peak current responses to pressure-applied 5-HT (10 μM) were recorded at steady holding potentials closely bracketing $E_{5\text{-}HT}$, which was subsequently

determined by interpolation. The two methods gave similar results.

Concentration-response relationships to 5-HT (0.3–100 μM) were determined from the peak inward whole-cell current response recorded in the presence of solutions E1 and I1 at a holding potential of −60 mV. The data were fitted iteratively using SigmaPlot 8 (Systat Software Inc., San Jose, CA) by an equation of the form

$$\frac{I}{I_{max}} = \left(\frac{[A]}{[A] + [EC_{50}]}\right)^{n_H} \quad \text{(Eq. 1)}$$

where I is the peak current elicited by 5-HT at concentration $[A]$, I_{max} is the peak current evoked by a saturating concentration of 5-HT, EC_{50} is the concentration of 5-HT that evokes a half-maximal response, and n_H is the Hill coefficient. To combine the concentration-response data obtained from several cells, agonist-evoked currents were normalized and expressed as a percentage of the maximal inward current response produced by a saturating concentration of 5-HT obtained for each cell.

Single channel currents evoked by pressure application of 5-HT (10 μM) were recorded from excised outside-out membrane patches clamped at steady holding potentials within the range of −100 to +100 mV as specified under "Results." The solutions used in such experiments were I1 and E1, E2, and E3, as appropriate. Additionally, in experiments that determined $E_{5\text{-HT}}$ and single channel conductance in mixtures of extracellular Na^+ and Ca^{2+}, NaCl was held at a constant concentration of 95 mM in the presence of variable concentrations of $CaCl_2$ (10^{-8}–3×10^{-2} M), sucrose (0–90 mM, as appropriate to maintain constant osmolarity), glucose (10 mM), and L-histidine (5 mM; pH 7.2). Currents were recorded using an Axopatch-1D amplifier (Axon Instruments, Union City, CA), low pass-filtered (5 KHz, Bessel characteristic), and recorded onto magnetic tape using a Bio-Logic DAT recorder (Bio-Logic, Claix, France) for subsequent offline analysis.

Data Analysis—Permeability ratios (relative to Cs^+) were determined from measurements of $E_{5\text{-HT}}$ and calculated ion activities (*i.e.* the ionic concentration multiplied by ion activity coefficient (γ_{ion})). The latter were estimated (following the Guggenheim convention) to be: γ_{Cs} 0.72 (140 mM Cs^+) γ_{Na} 0.76 (140 mM Na^+), and γ_{Ca} 0.26 (100 mM Ca^{2+}). For varying concentrations of Ca^{2+} in the presence of 95 mM Na^+, the mean molal activity coefficients for $CaCl_2$ in the presence of 100 mM NaCl, as tabulated by Butler (36), allowed calculation of γ_{Ca}. Sucrose had a negligible influence upon γ_{Na} over the range of sugar concentrations employed (37). The permeability ratio P_{Na}/P_{Cs} was calculated from the Goldman-Hodgkin-Katz (voltage) equation,

$$E_{5\text{-HT}} = \frac{RT}{F} \ln \frac{(P_{Na}/P_{Cs})[Na^+]_o}{[Cs^+]_i} \quad \text{(Eq. 2)}$$

where R, T, and F have their usual meaning and $[Na^+]_o$ and $[Cs^+]_i$ are the calculated activities of extracellular Na^+ and internal Cs^+ ions, respectively. This equation ignores the very small error anticipated due to the presence of low concentrations of permeant divalent ions (*e.g.* Ca^{2+}) within the extra- or intracellular solutions.

The permeability ratio, P_{Ca}/P_{Cs}, was calculated from a modified Goldman-Hodgkin-Katz (voltage) equation (38) which, with both Na^+ and Ca^{2+} present as permeant species in the extracellular medium but only Cs^+ and negligible Ca^{2+} present in the pipette ('intracellular') solution, can be written as (20)

$$E_{5\text{-HT}} = \frac{RT}{F} \ln \frac{P_{Na}/P_{Cs}[Na^+]_o + 4(P'_{Ca}/P_{Cs})[Ca^{2+}]_o}{[Cs^+]_i} \quad \text{(Eq. 3)}$$

where $[Na^+]_o$ and $[Ca^{2+}]_o$ are the external activities of Na^+ and Ca^{2+}, $[Cs^+]_i$ is the internal activity of Cs^+, and P'_{Ca}/P_{Cs} is a modified term relating the permeability of Ca^{2+} to Cs^+. Substituting for P'_{Ca}/P_{Cs}, the above can also be written as

$$\exp^{E_{5\text{-HT}}F/RT} = \frac{P_{Na}[Na^+]_o}{P_{Cs}[Cs^+]_i} + 4\frac{P_{Ca}[Ca^{2+}]_o}{P_{Cs}(1 + \exp^{E_{5\text{-HT}}F/RT})[Cs^+]_i} \quad \text{(Eq. 4)}$$

When Ca^{2+} was the sole cation in the extracellular medium, the term P_{Na}/P_{Cs} was omitted. For simplicity, in the text we routinely refer to ion concentrations (in square brackets) rather than activities (in parentheses), although the latter were used in all calculations of relative permeability and are presented in the figures where relevant.

Single channel currents were low pass-filtered offline at 1 KHz, digitized at 10 KHz via a DigiData 1302A (Axon Instruments) interface. Using the WinEDR V2 7.6 electrophysiology data recorder (J. Dempster, Dept. of Physiology and Pharmacology, University of Strathclyde, UK), single channel current amplitude histograms were constructed from sections of single channel activity in which unitary events predominated. A transition detection threshold of 30–40% of the predominant unitary event amplitude was employed to capture events for inclusion within the amplitude histogram. Events less than 1 ms in duration (classified as incompletely resolved), obvious artifacts, and those corresponding to multiple openings were rejected. The resulting mean open state amplitude histogram was fitted using an iterative least squares algorithm with a single Gaussian probability density function from which unitary event amplitude (i) was determined. The analysis was restricted to the dominant unitary current state, as events of differing amplitude were relatively rare. Single channel conductance (γ) is routinely reported as the chord conductance, *i.e.* $\gamma = i/(V_m - E_{5\text{-HT}})$, where V_m is the holding potential (including liquid junction potential correction) and $E_{5\text{-HT}}$ is the reversal potential of the agonist-evoked macroscopic response determined as described above under the appropriate ionic conditions.

Statistical Analysis—Data are presented as mean ± S.E. Statistical analysis was conducted using one-way analysis of variance with the post hoc Dunnett or Tukey test as appropriate. A value of $p < 0.05$ was considered significant.

RESULTS

Residues in the MA helix of the 5-HT_{3A} Receptor Influence Ca^{2+} Permeability—We recently demonstrated that arginine residues 432, 436, and 440 within the MA helix motif of the

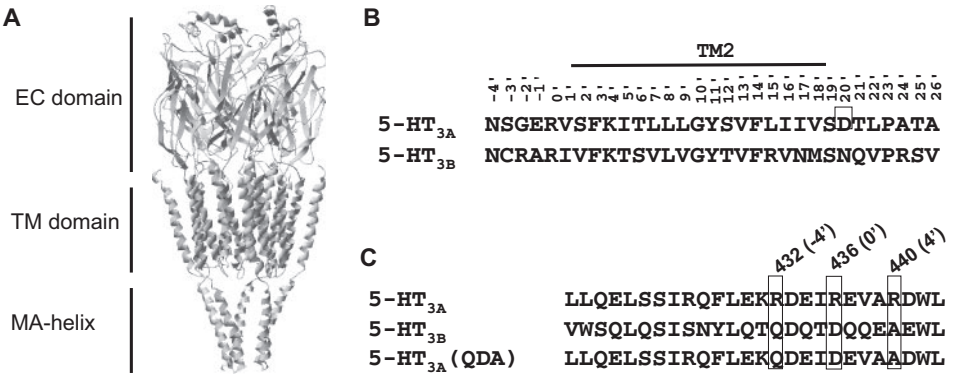

FIGURE 1. **Domains of the 5-HT_3 receptor that influence ion conduction and selectivity between mono- and divalent cations.** *A*, homology model of the wild-type 5-HT_{3A} receptor using the nicotinic ACh receptor of *Torpedo marmorata* as a template (32). The functional modules are denoted: extracellular domain (*EC*), pore-forming transmembrane helices (*TM*), and the portal-framing cytoplasmic MA helices (*MA*). *B*, sequence alignment of the second transmembrane domain (*TM2*) and flanking sequences of the human 5-HT_{3A} and 5-HT_{3B} subunits. The residue mutated to alanine in the mutant 5-HT_{3A} receptor constructs is *boxed*. *C*, an alignment of amino acids within the MA helices of wild-type 5-HT_{3A} and 5-HT_{3B} subunits and the mutant 5-HT_{3A}(QDA) construct used in this study, indicating the positions of the −4′, 0′, and 4′ residues (*boxed*). Amino acids are numbered according to the human 5-HT_{3A} subunit amino acid sequence (51).

TM3–4 loop at positions termed MA −4′, 0′, and 4′, respectively, which line putative cytoplasmic portals (Fig. 1*C*), are responsible for the sub-pS single channel conductance of the 5-HT_{3A} receptor (2, 22, 31). We began this study by testing the hypothesis that the same 5-HT_{3A} MA helix arginine residues also serve as determinants of ionic selectivity.

The relative permeability ratio, P_{Na}/P_{Cs}, of wild-type and mutant 5-HT_{3A} receptors was calculated by determining $E_{5\text{-HT}}$ from voltage ramps (−100 to +60 mV) that coincided with the peak of the macroscopic current response to pressure-applied 5-HT in the presence of extracellular and intracellular electrolytes E2 and I1, respectively (Fig. 2*A*). Ramp currents generated in the absence of 5-HT were subtracted from ramp currents in the presence of 5-HT yielding an inwardly rectifying *I-V* relationship with an $E_{5\text{-HT}}$ of 2.1 ± 0.7 mV, corresponding to a P_{Na}/P_{Cs} ratio of 1.02 ± 0.03 ($n = 15$; Figs. 2*B* and 3*A*, Table 1) for the wild-type receptor. In six cells from this population, $E_{5\text{-HT}}$ was redetermined following the exchange of solution E2 with E3 (*i.e.* complete replacement of Na^+ by 100 mM Ca^{2+}), resulting in a negative shift in $E_{5\text{-HT}}$ to −6.1 ± 1.3 mV accompanied by a pronounced depression in the amplitude of the 5-HT-evoked current and the loss of inward rectification in the *I-V* relationship, most noticeable at positive potentials (Fig. 2*B*). Despite substantial inhibition of current amplitude by extracellular Ca^{2+}, P_{Ca}/P_{Cs} (1.42 ± 0.11, $n = 6$; Fig. 3*A*, Table 1) was greater than P_{Na}/P_{Cs} ($p = 0.021$, paired *t* test).

Experiments performed on the 5-HT_{3A}(QDA) mutant using the voltage ramp protocol yielded a P_{Na}/P_{Cs} ratio of 0.9 ± 0.04 ($E_{5\text{-HT}} = -1.3 \pm 1.0$ mV, $n = 13$), which is not significantly different from that of the wild-type 5-HT_{3A} receptor (Fig. 2*C*, Table 1). An essentially identical value for $E_{5\text{-HT}}$ (−1.4 ± 0.5 mV, $n = 3$) was found from measurements of 5-HT-induced peak current amplitudes at potentials closely bracketing that of current reversal. However, in contrast to the negative shift in $E_{5\text{-HT}}$ found for the wild-type 5-HT_{3A} receptor upon replacement of solution E2 by E3, that of the mutant displayed a robust positive shift to 9.4 ± 1.4 mV ($n = 10$), reflecting a significant increase in P_{Ca}/P_{Cs} to 3.65 ± 0.34 ($n = 10$, Figs. 2*C* and 3*A*, Table 1). Despite the enhancement of P_{Ca}/P_{Cs} at the 5-HT_{3A}(QDA) receptor, inhibition of the macroscopic current responses by extracellular Ca^{2+} persisted, although the effect was less pronounced at positive potentials due to the outward, *versus* mild inward, rectification typically observed in the Ca^{2+}- and Na^+-containing extracellular solutions, respectively (Fig. 2*C*).

In subsequent experiments, we evaluated the contributions of the individual mutations R432Q (MA −4′), R436D (MA 0′), and R440A (MA 4′) to the enhancement of P_{Ca}/P_{Cs}. The R436D charge reversal mutation produces an ~6-fold increase in single channel conductance compared with the wild-type 5-HT_{3A} receptor (22). The 5-HT_{3A}(R436D) receptor also had a significantly enhanced relative permeability to Ca^{2+} ($P_{Ca}/P_{Cs} = 3.13 \pm 0.31$, $n = 7$, Fig. 3*A*, Table 1). By contrast, the introduction of aspartate did not significantly affect P_{Na}/P_{Cs} compared with wild-type 5-HT_{3A} receptors (Fig. 3*A*, Table 1). Notably, the P_{Ca}/P_{Cs} of the 5-HT_{3A}(QDA) receptor was not significantly greater than that of the 5-HT_{3A}(R436D) receptor. The individual replacement of Arg-432 by the equivalent 5-HT_{3B} subunit residue glutamine had no significant effect on single channel conductance (22). Likewise, the permeability of Ca^{2+} relative to Cs^+ of the 5-HT_{3A}(R432Q) mutant was similar to that of the wild-type 5-HT_{3A} receptor, suggesting that this MA helix residue has little influence on ion selectivity (Fig. 3*A*, Table 1). Substitution of Arg-440 residue by alanine significantly increased single channel conductance (22). Although the 5-HT_{3A}(R440A) mutant exhibited a trend toward an increased P_{Ca}/P_{Cs} ratio relative to the wild-type receptor, the effect failed to reach statistical significance (Fig. 3*A*, Table 1).

The validity of the above estimates of P_{Na}/P_{Cs} and P_{Ca}/P_{Cs} for the 5-HT_{3A}(QDA) receptor construct relies upon the mutant retaining the near perfect cation *versus* anion selectivity of the wild-type receptor ($P_{Na}/P_{Cl} = 53$) (30). We tested this assumption rigorously by dilution experiments in which the NaCl content of the extracellular solution E2 was reduced to 95, 50, and 20 mM by replacement with sucrose. Under such conditions a plot of $E_{5\text{-HT}}$ as a function of the logarithm of extracellular Na^+ activity, $(Na^+)_o$, was linear and yielded a slope of 59 mV/decade change in $(Na^+)_o$ (Fig. 3*B*). A similar dependence upon $(Na^+)_o$ was observed under simplified bi-ionic conditions in which Na^+ totally replaced Cs^+ within the intracellular solution. Because only a slope of less than 58 mV/decade change in $(Na^+)_o$ is compatible with anion permeation (28), we concluded that for the 5-HT_{3A}(QDA) receptor construct $P_{Na}/P_{Cl} = \infty$.

The foregoing results indicate that the arginine residues present at positions 436 (MA 0′) and to a lesser extent 440 (MA 4′) of the human wild-type 5-HT_{3A} receptor collectively suppress the permeability of Ca^{2+}, but not Na^+, relative to Cs^+, revealing that the large intracellular loop of a Cys-loop receptor

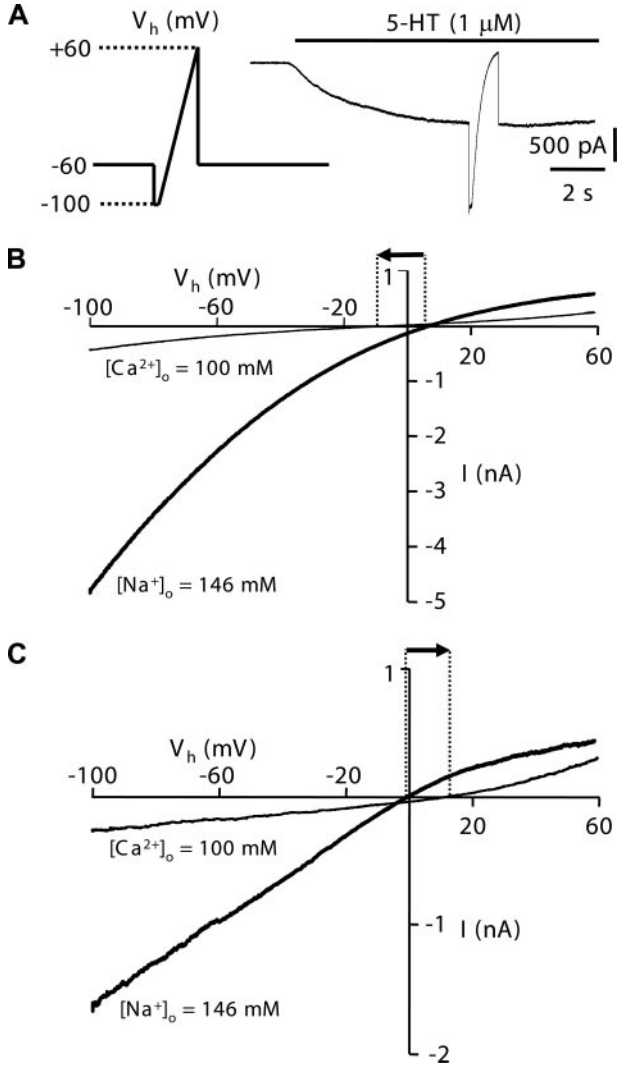

FIGURE 2. **The reversal potential of 5-HT-evoked macroscopic currents at wild-type 5-HT_{3A} and 5-HT_{3A}(QDA) receptor constructs with Na^+ or Ca^{2+} as the charge carrier in the extracellular solution.** *A*, voltage ramp (*left*) applied at the peak of the macroscopic inward current response to pressure-applied 5-HT (1 μM) (*right*) to determine the reversal potential ($E_{5\text{-HT}}$) of the agonist-induced response mediated by the wild-type 5-HT_{3A} receptor. *B*, current-voltage relationships recorded from a representative HEK-293 cell expressing the wild-type 5-HT_{3A} receptor with an intracellular CsCl-based solution (I1) as reference and NaCl (146 mM)-based solution E2 or $CaCl_2$ (100 mM)-based solution E3 as the extracellular electrolyte. Note the negative shift in $E_{5\text{-HT}}$ (*arrow*) upon complete iso-osmotic replacement of extracellular Na^+ by Ca^{2+}. *C*, current-voltage relationships recorded from a representative HEK-293 cell expressing the 5-HT_{3A}(QDA) receptor under the conditions described in *B*. Note that complete iso-osmotic replacement of extracellular Na^+ by Ca^{2+} causes a positive shift in $E_{5\text{-HT}}$ (*arrow*).

is an important determinant of divalent *versus* monovalent cation selectivity.

The Charge of the MA stretch 0′ Residue Is the Principal Determinant of Ca^{2+} Permeability—We further evaluated the influence of charge at the MA 0′ position by determining P_{Ca}/P_{Cs} for constructs in which the residue was either negative (5-HT_{3A}(R432Q, R436E, R440A); abbreviated as 5-HT_{3A}(QEA)), neutral (5-HT_{3A}(R432Q, R436A, R440A) and 5-HT_{3A}(R432Q, R436F, R440A); abbreviated as 5-HT_{3A}(QAA) and 5-HT_{3A}(QFA), respectively), or remained positive (5-HT_{3A}(R432Q, R440A); abbreviated as 5-HT_{3A}(QRA)). P_{Ca}/P_{Cs} was significantly enhanced compared with the wild-type

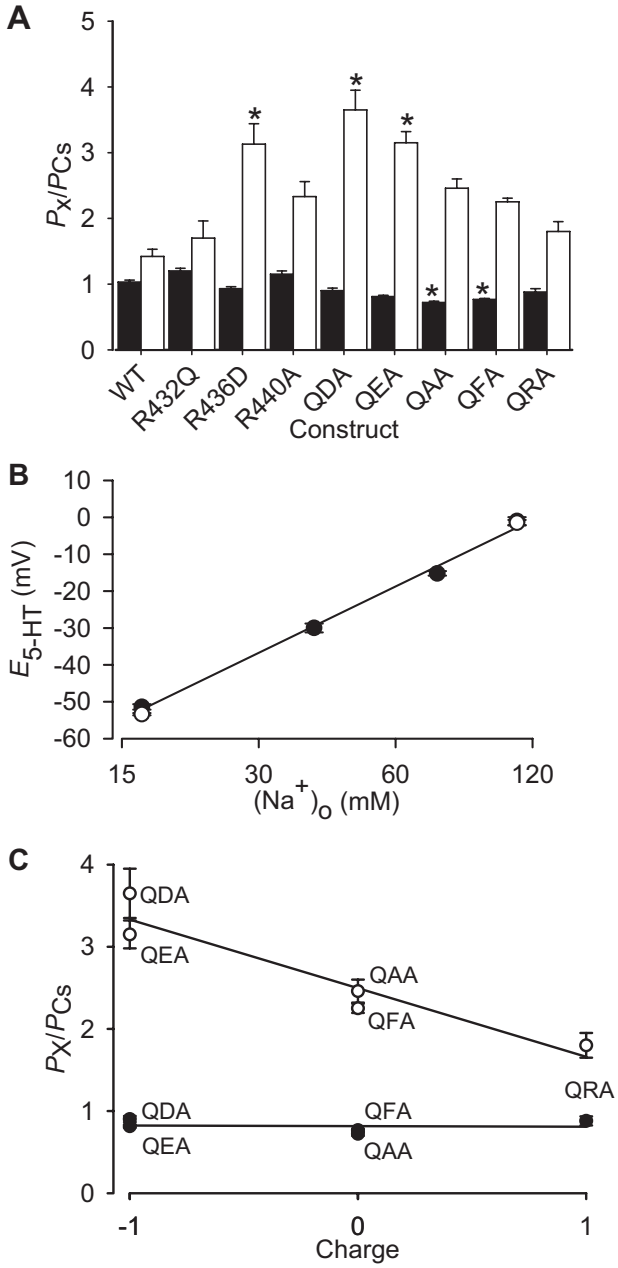

FIGURE 3. **Comparison of the relative ion permeability of wild-type and mutant 5-HT_{3A} receptor constructs.** *A*, bar graph illustrating the relative permeability (P_x/P_{Cs}) of Na^+ (*black bars*), or Ca^{2+} (*white bars*) relative to Cs^+ for the indicated receptor constructs. Permeability ratios were determined with I1 as the intracellular reference solution and NaCl (146 mM)-based solution E2 or $CaCl_2$ (100 mM)-based solution E3 as the extracellular electrolyte. Data are the mean ± S.E. of 5–17 independent estimates of P_x/P_{Cs} performed from separate cells. Mutant constructs in which P_{Na}/P_{Cs} or P_{Ca}/P_{Cs} was significantly different from the appropriate wild-type control are indicated with an *asterisk* ($p < 0.05$; analysis of variance followed by Dunnett's post hoc test). *B*, relationship between the reversal potential of the macroscopic current evoked by 5-HT ($E_{5\text{-HT}}$) and the activity of Na^+ in the extracellular medium ($(Na^+)_o$) for the 5-HT_{3A}(QDA) receptor construct. Responses were recorded with extracellular electrolytes based on solution E2 wherein the concentration of NaCl was reduced by substitution with sucrose. Intracellular solutions were either CsCl-based I1 (*filled circles*) or a solution in which NaCl totally replaced CsCl (*open circles*) to produce bi-ionic recording conditions. The regression line fitted to the *filled circles* yielded a slope of 59 mV/decade change in $(Na^+)_o$. Data points are the mean of 3–6 independent determinations of $E_{5\text{-HT}}$, and *vertical bars* indicate ± S.E. *C*, relationship between P_{Na}/P_{Cs} (*filled circles*) and P_{Ca}/P_{Cs} (*open circles*) and the charge of the amino acid residue at position 436 of the MA helix.

TABLE 1

The influence of mutations within the intracellular MA helix upon the permeabilities of Ca^{2+} and Na^+ relative to Cs^+

Relative permeabilities (*i.e.* P_{Ca}/P_{Cs} and P_{Na}/P_{Cs}) were calculated from determinations of $E_{5\text{-HT}}$ in extracellular solutions containing Na^+ (solution E2) or Ca^{2+} (solution E3) as the permeant cation. Statistical significance was determined by analysis of variance with Dunnett's post hoc test. *, indicates significantly different from the appropriate wild-type permeability ratio, $p < 0.01$. WT, wild-type; QDA, 5-HT_{3A}(R432Q,R436D,R440A); QEA, 5-HT_{3A} (R432Q, R436E, R440A); QAA, 5-HT_{3A}(R432Q,R436A,R440A); QFA, (5-HT_{3A}(R432Q,R436F,R440A); QRA, 5-HT_{3A}(R432Q,R440A).

5-HT_{3A} constructs	Na^+ extracellular			Ca^{2+} extracellular		
	$E_{5\text{-HT}}$	P_{Na}/P_{Cs}	*n*	$E_{5\text{-HT}}$	P_{Ca}/P_{Cs}	*n*
	mV			*mV*		
WT 5-HT_{3A}	2.1 ± 0.7	1.03 ± 0.03	15	−6.1 ± 1.3	1.42 ± 0.11	6
R432Q	6.0 ± 0.9	1.20 ± 0.04	17	−3.4 ± 2.6	1.70 ± 0.26	7
R436D	−0.4 ± 0.7	0.93 ± 0.03	13	7.1 ± 1.4	3.13 ± 0.31*	7
R440A	4.8 ± 1.1	1.15 ± 0.05	5	2.3 ± 1.7	2.33 ± 0.23	5
QDA	−1.3 ± 1.0	0.90 ± 0.04	10	9.4 ± 1.4	3.65 ± 0.30*	10
QEA	−3.6 ± 0.6	0.81 ± 0.02	4	7.6 ± 0.9	3.15 ± 0.17*	4
QAA	−6.8 ± 0.9	0.72 ± 0.02*	8	3.5 ± 0.9	2.46 ± 0.14	6
QFA	−5.2 ± 0.5	0.77 ± 0.01*	8	2.1 ± 0.4	2.25 ± 0.06	5
QRA	−2.0 ± 1.6	0.88 ± 0.05	7	−2.1 ± 1.4	1.80 ± 0.15	7

5-HT_{3A} receptor for the 5-HT_{3A}(QEA) construct. The enhancement observed for the 5-HT_{3A}(QEA) construct was not significantly different from that found for the 5-HT_{3A}(QDA) receptor. Although P_{Ca}/P_{Cs} was not significantly different from the wild-type 5-HT_{3A} receptor for the 5-HT_{3A}(QAA), 5-HT_{3A}(QFA), and 5-HT_{3A}(QRA) constructs, the ratio tended to decrease progressively as the charge at position 436 changed from negative, through neutral, to positive (Fig. 3, *A* and *C*, Table 1). Thus, charge inversion appears necessary to cause a shift in $E_{5\text{-HT}}$ sufficient to produce a statistically significant difference in P_{Ca}/P_{Cs} values. Finally, measurements of $E_{5\text{-HT}}$ with Na^+ as the predominant extracellular cation revealed no significant change in P_{Na}/P_{Cs} relative to the wild-type receptor, apart from the 5-HT_{3A}(QAA) and 5-HT_{3A}(QFA) constructs in which the ratio was modestly reduced to 0.72 ± 0.02 and 0.77 ± 0.01, respectively (Fig. 3, *A* and *C*, Table 1). Despite the latter finding, the sign of the charge at position 436 clearly had no consistent influence upon P_{Na}/P_{Cs} (Fig. 3*C*). In aggregate, the results suggest that the reversal of charge at position 436 within the 5-HT_{3A}(QDA) construct was the predominant cause of a greatly increased P_{Ca}/P_{Cs} relative to the wild-type receptor.

The 5-HT_{3A}(QDA) Receptor Conducts Ca^{2+} Less Efficiently than Na^+—Determinations of relative permeability based on reversal potential measurements do not predict the relative ease with which ion channels conduct permeant ions (39). For example, a binding site for Ca^{2+} within the permeation pathway may confer selectivity toward this divalent, yet retard its flux in comparison to monovalent cations. Indeed, we previously demonstrated that extracellular divalent cations (Mg^{2+} and Ca^{2+}) reduce the single channel conductance of the wild-type 5-HT_{3A} receptor as estimated using fluctuation analysis (20). However, the latter technique tends to underestimate single channel conductance, and it is preferable to measure single channel conductances directly using excised patch recording (22). This is impossible for the wild-type 5-HT_{3A} receptor, with a conductance of <1 pS, which is below the resolution of the patch-clamp technique (20, 21, 40). In contrast, the 5-HT_{3A}(QDA) construct has a single channel conductance that enables the direct resolution of single channel currents in outside-out patch recordings (slope conductance of 37 pS at −74 mV (22)).

With Na^+ as the predominant extracellular cation, the single channel current-voltage relationship (*i-V*) for the 5-HT_{3A} (QDA) receptor shows a very mild outward rectification over a wide range of holding potentials (−100 to 100 mV) and yields chord conductance levels of 46 and 40 pS at holding potentials of +100 and −100 mV, respectively (Fig. 4, *A* and *B*). The latter is slightly larger than previously reported by us (22); this minor difference is due to the reduced concentration of divalent cations in the extracellular medium E2. Inclusion of 1 mM Ca^{2+} and 2 mM Mg^{2+} (medium E1) also yielded an essentially linear *i-V* relationship but with a slope conductance corresponding to our previous estimate (22).

In contrast to the mild outward rectification of the *i-V* relationship observed with Na^+, when Ca^{2+} was the sole extracellular cation, 5-HT-evoked single channel events mediated by the 5-HT_{3A}(QDA) receptor displayed marked outward rectification (Fig. 4, *A* and *B*) similar to that seen in whole-cell current recordings (Fig. 2*C*). At all negative holding potentials, single channel current amplitudes were greatly reduced in comparison to when Na^+ was the permeant cation. At the most negative potential studied (−100 mV), where it can be assumed that single channel currents reflect inward movement of Ca^{2+} with little opposing outwardly directed monovalent cation flux, a single channel chord conductance of 5.7 pS was calculated, assuming an $E_{5\text{-HT}}$ of 9.4 mV obtained from macroscopic currents recorded under identical ionic conditions. The disparity between single channel current amplitudes recorded in Na^+- and Ca^{2+}-containing solutions decreased as the holding potential was progressively shifted to more positive values (Fig. 4, *A* and *B*). This is most clearly appreciated by inspection of Fig. 4*C*, which plots unitary current amplitude against driving force (*i.e.* holding potential *minus* $E_{5\text{-HT}}$). Indeed, at the most positive potentials examined, where an outwardly directed flux of Cs^+ predominates, single channel current amplitudes were indistinguishable between Na^+- and Ca^{2+} - based extracellular solutions (Fig. 4*C*). The data indicate that the 5-HT_{3A}(QDA) receptor construct, despite selecting for Ca^{2+} over Na^+, conducts the former less efficiently, thus predicting that extracellular Ca^{2+} will (at negative holding potentials) reduce single channel conductance in mixtures of Na^+ and Ca^{2+} as we previously inferred for the human wild-type 5-HT_{3A} receptor by fluctuation analysis (20).

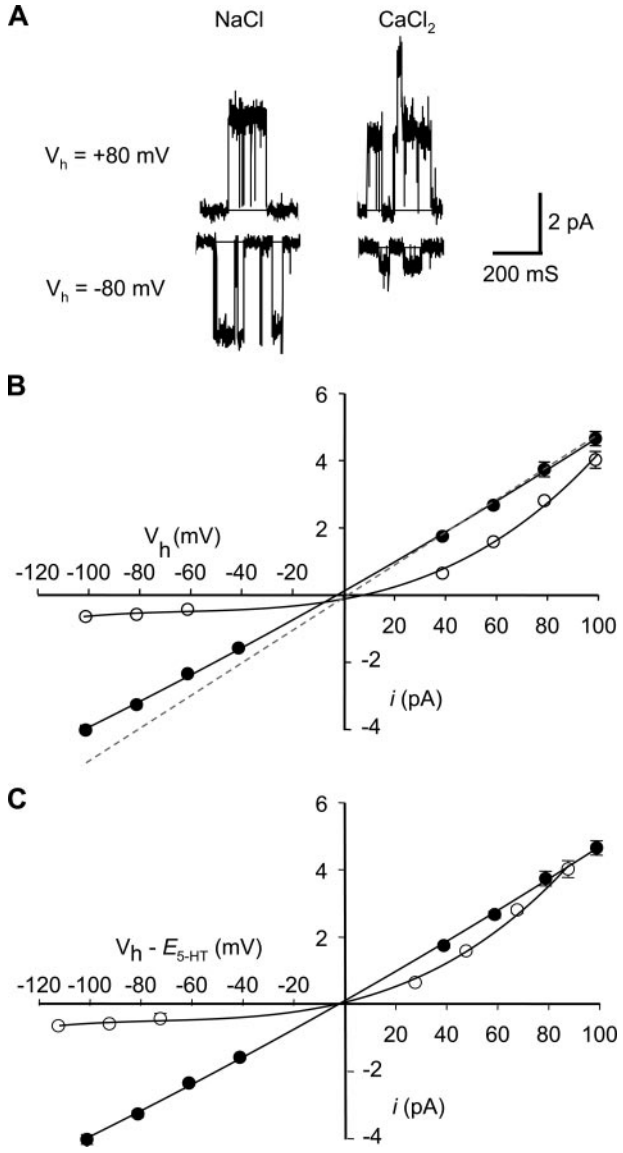

FIGURE 4. **Single channel currents mediated by the 5-HT_{3A}(QDA) receptor construct with Na^+ or Ca^{2+} as the extracellular permeant ion species.** Single channel currents (*i*) were recorded from outside-out membrane patches in response to pressure-applied 5-HT (10 μM) at holding potentials (V_h) ranging from −100 to +100 mV. The patch pipette contained CsCl-based solution I1, and the patch was superfused with NaCl (146 mM)-based solution E2 or $CaCl_2$ (100 mM)-based solution E3. *A*, exemplar single channel currents with either Na^+ (*left*) or Ca^{2+} (*right*) as the extracellular permeant cation. *B*, current-voltage (*i-V*) plot for single channel currents recorded with NaCl-based solution E2 (*filled circles*) or $CaCl_2$-based solution E3 (*open circles*) as the extracellular electrolyte. Note the mild outward rectification with Na^+ as the permeant ion species in the extracellular medium (compare *dashed line* fitted to data obtained at positive potentials to *curve* fitted to all data points). By contrast, marked outward rectification is evident when $CaCl_2$ totally replaces NaCl. *C*, *i-V* plot depicted in *B* but with driving force (*i.e.* $V_h - E_{5\text{-HT}}$) replacing V_h on the *abscissa*. $E_{5\text{-HT}}$ was determined from macroscopic current responses to 5-HT (see "Experimental Procedures"). The plot reveals that outwardly directed single channel current amplitudes, at the most positive V_h values examined, are essentially identical in Na^+- and Ca^{2+}-containing extracellular solutions when equivalent driving forces are considered. Each data point in *B* and *C* is the mean of 3–10 determinations of single channel current amplitude derived from different outside-out membrane patches. The *vertical bars*, when exceeding the size of the *symbols*, indicate ± S.E.

Extracellular Ca^{2+} Reduces the Single Channel Conductance of the 5-HT_{3A}(QDA) Receptor in a Concentration-dependent Fashion—We examined the influence of extracellular Ca^{2+} upon the single channel conductance of the 5-HT_{3A}(QDA) receptor construct with an extracellular solution containing 95 mM Na^+ and varying concentrations of Ca^{2+} (10 nM to 30 mM). Chord conductances were derived from single channel current amplitudes recorded at a holding potential of −80 mV, and measurements of $E_{5\text{-HT}}$ were made from macroscopic currents in the ionic mixtures. In this series of experiments, $E_{5\text{-HT}}$ was estimated by interpolation between the peak amplitude of inwardly and outwardly directed 5-HT-induced currents that closely bracketed the zero current potential. Consistent with the relative permeability measurements made with high Ca^{2+} solution (E3, Table 1), the addition of increasing concentrations of Ca^{2+} was associated with a progressive shift in $E_{5\text{-HT}}$ to more positive values (from −15.0 ± 0.04 mV (n = 4) with $[Ca^{2+}]_o$ = 0.1 mM to −1.6 ± 0.7 mV (n = 3) with $[Ca^{2+}]_o$ = 30 mM; Fig. 5*A*). Single channel conductance was reduced by ~65% over the range $[Ca^{2+}]_o$ = 0.1 mM (41.3 ± 0.88 pS) to $[Ca^{2+}]_o$ = 30 mM (14.8 ± 0.63 pS; Fig. 5, *B* and *C*). However, it should be noted that Ca^{2+} will itself contribute to inward current amplitude, particularly at high $[Ca^{2+}]_o$. For this reason the calculation of an IC_{50} value for the suppressant effect of Ca^{2+} upon single channel conductance was inappropriate. A simple interpretation of such data is that Ca^{2+} reduces single channel conductance by binding to a site(s) of comparatively low affinity within the permeation pathway and thereby occludes the flux of Na^+. In agreement with such a violation of the independent movement of Na^+ and Ca^{2+} within the permeation pathway, the ratio P_{Ca}/P_{Cs} was found to be concentration-dependent. With $[Na^+]_o$ fixed at 95 mM (and assuming P_{Na}/P_{Cs} = 0.9; see above), P_{Ca}/P_{Cs} was calculated from determinations of $E_{5\text{-HT}}$ to be 0.5 and 1.8 in the presence of 10 and 30 mM extracellular Ca^{2+}, respectively, *versus* the value of 3.7 found with Ca^{2+} as the sole extracellular charge carrier.

Extracellular Ca^{2+} Reduces Single Channel Conductance of the 5-HT_{3A}(QDA) Receptor in a Voltage-independent Manner—Blockade by Ca^{2+} of macroscopic current responses mediated by the 5-HT_{3A} receptor expressed in mammalian cell hosts is voltage-independent (20, 21, 34, 40, 41). The readily resolvable single channel conductance of the 5-HT_{3A}(QDA) receptor allowed direct measurements of the influence of extracellular Ca^{2+} upon single channel current amplitudes over a range of membrane potentials. Fig. 6 depicts the results of such studies where $[Ca^{2+}]_o$ was varied between 0.3 and 10 mM in the presence of 95 mM Na^+ and single channel events evoked by pressure-applied 5-HT (10 μM) were recorded from outside-out membrane patches at holding potentials in the range of −40 to −100 mV. At all concentrations of extracellular Ca^{2+} studied the single channel *i-V* relationship was well fitted by a linear function and showed no evidence of a region of negative slope conductance or outward rectification (Fig. 6). In addition, the single channel conductances derived from the slope of the *i-V* relationships (*i.e.* 35.8, 29.4, 25.0, and 20.0 pS in the presence of 0.3, 1, 3, and 10 mM Ca^{2+}, respectively) were in excellent agreement with the chord conductances reported in Fig. 5*C*. Thus, the reduction in single channel conductance by extracellular Ca^{2+} is voltage-independent over the range of negative potentials examined.

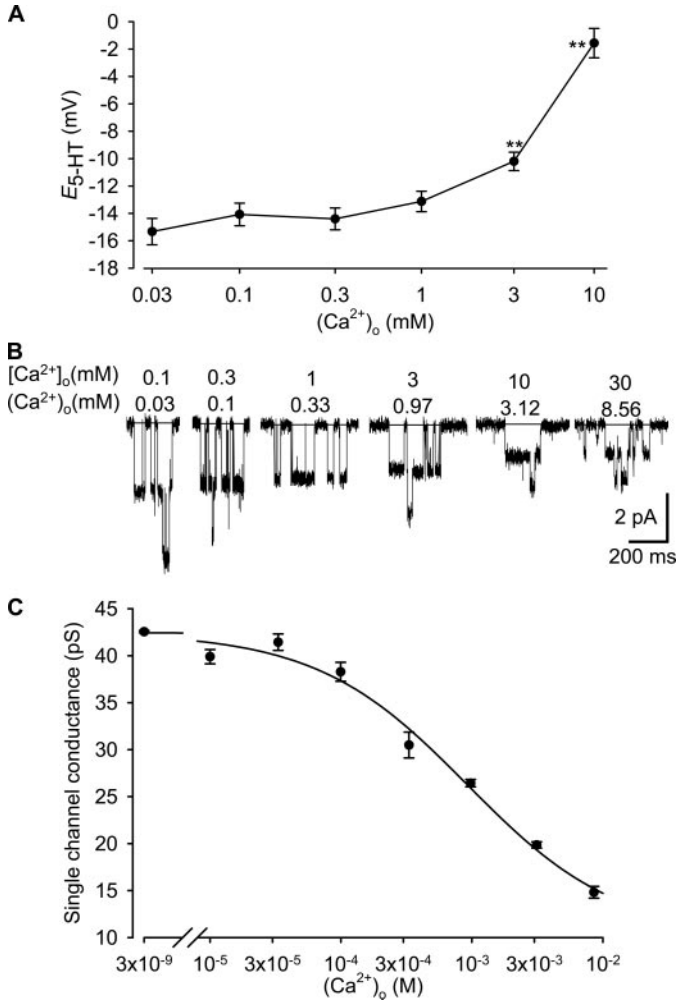

FIGURE 5. **Extracellular Ca^{2+} depresses the single channel conductance of the 5-HT_{3A}(QDA) receptor construct.** *A*, reversal potential of the macroscopic current response to 5-HT ($E_{5\text{-HT}}$) with $[Na^+]_o$ set to 95 mM and $[Ca^{2+}]_o$ within the range of 0.1 to 30 mM. Note that Ca^{2+} ion activity, $(Ca^{2+})_o$, rather than concentration, $[Ca^{2+}]_o$, is plotted in *A* and *C*. Data are the mean of 3–4 observations, and *vertical bars* indicate S.E. **, $p < 0.01$ as determined by analysis of variance followed by Dunnett's post hoc test. *B*, single channel currents in response to 5-HT (10 μM) applied by pressure to outside-out membrane patches voltage-clamped at a holding potential (V_h) of −80 mV. Increasing $[Ca^{2+}]_o$ depresses unitary current amplitude in a concentration-dependent manner. Note that an increased driving force (*i.e.* $V_h - E_{5\text{-HT}}$) when $[Ca^{2+}]_o$ is equal to 10 and 30 mM (corresponding to a $(Ca^{2+})_o$ of 3.12 and 8.56 mM, respectively; see *A*) partially masks the magnitude of the suppression of single channel current amplitudes by Ca^{2+}. *C*, concentration-response relationship illustrating the depressant effect of extracellular Ca^{2+} upon single channel conductance. Data are the mean ± S.E. of measurements performed on 4–5 outside-out membrane patches under the conditions described in *B*.

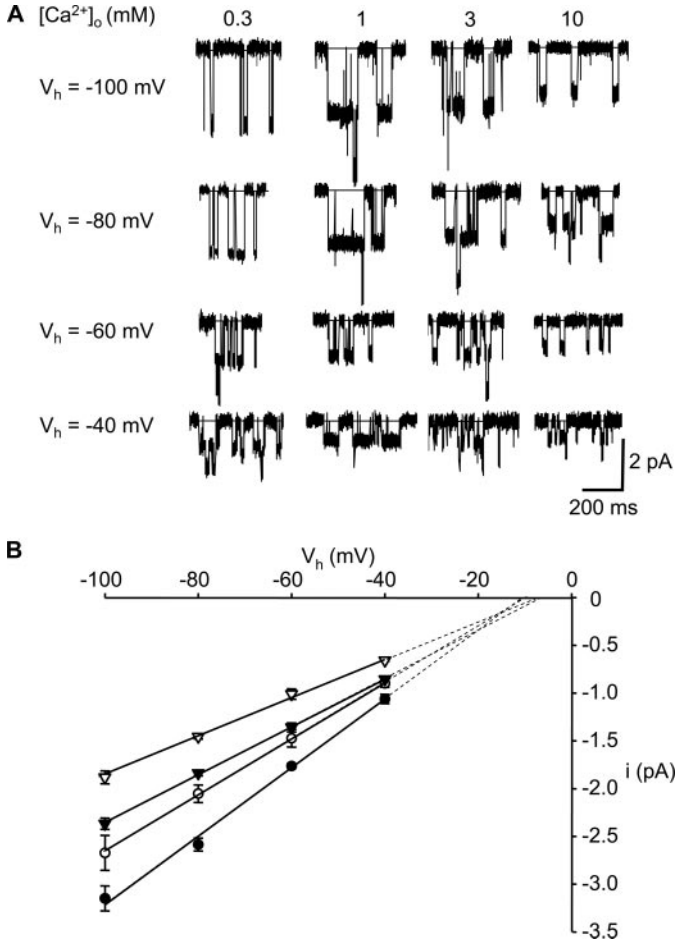

FIGURE 6. **Extracellular Ca^{2+} reduces the single channel conductance of the 5-HT_{3A}(QDA) receptor construct in a manner independent of transmembrane potential.** *A*, single channel currents recorded from outside-out membrane patches in response to pressure-applied 5-HT (10 μM). The currents were recorded at holding potentials in the range of −100 to −40 mV in the presence of 0.3, 1, 3, or 10 mM extracellular Ca^{2+} and 95 mM Na^+. *B*, *i-V* relationships for single channel events recorded with $[Na^+]_o$ constant at 95 mM and $[Ca^{2+}]_o$ present at 0.3 mM (*filled circles*), 1 mM (*open circles*), 3 mM (*filled inverted triangles*), or 10 mM (*open inverted triangles*). The relationship between single channel current amplitude and V_h at each concentration of Ca^{2+} was fitted by linear regression analysis to yield slope conductance values of 35.8, 29.4, 25.0, and 20.0 pS in the presence of 0.3, 1, 3, and 10 mM Ca^{2+}, respectively. *Dashed lines* represent an extrapolation of each *i-V* plot to the zero current level ($E_{5\text{-HT}}$). Each data point is the mean of single channel current amplitudes derived from recordings performed on 3–5 outside-out membrane patches, and the *vertical bars* indicate ± S.E.

Extracellular Na^+ Influences Reduction of the Single Channel Conductance of the 5-HT_{3A}(QDA) Receptor by Extracellular Ca^{2+} and Mg^{2+}—The single channel conductance of the 5-HT_{3A}(QDA) receptor decreased from 41.1 to 26.5 pS when $[Ca^{2+}]_o$ was elevated from 0.1 to 3 mM in an extracellular solution containing 95 mM Na^+ (Fig. 5*C*). However, only a modest decrease in single channel conductance (*i.e.* from 40.8 to 35.7 pS) occurred when solution E1 (containing 1.0 mM Ca^{2+} and 2.0 mM Mg^{2+} in the presence of 140 mM Na^+) replaced solution E2 (containing 0.1 mM Ca^{2+} and 0.1 mM Mg^{2+} in the presence of 140 mM Na^+). The 5-pS decrease in conductance is far less than that predicted (11 pS) from Fig. 5*C* when $[Ca^{2+}]_o$ was increased from 0.1 to 1.0 mM, even neglecting a likely contribution from Mg^{2+} (20, 40). The reason for this apparent discrepancy is an interaction between $[Na^+]_o$ and $[cation^{2+}]_o$ (Fig. 7). In solutions where $[Na^+]_o$ was set at 140, 95, and 50 mM Na^+ (osmolarity maintained with sucrose), single channel chord conductance recorded at a holding potential of −80 mV in the presence of 0.1 mM each Ca^{2+} and Mg^{2+} was unchanged between the 140 and 95 mM solutions but was significantly depressed in the 50 mM solution (range 40.8 to 34.4 pS; Fig. 7). However, in similar solutions containing 1 mM Ca^{2+} and 2 mM Mg^{2+}, single channel conductance decreased markedly in parallel with diminished $[Na^+]_o$ (range, 35.7 to 18.3 pS; Fig. 7). The data are consistent with competition between Na^+ and divalent cations for a binding site within the permeation pathway.

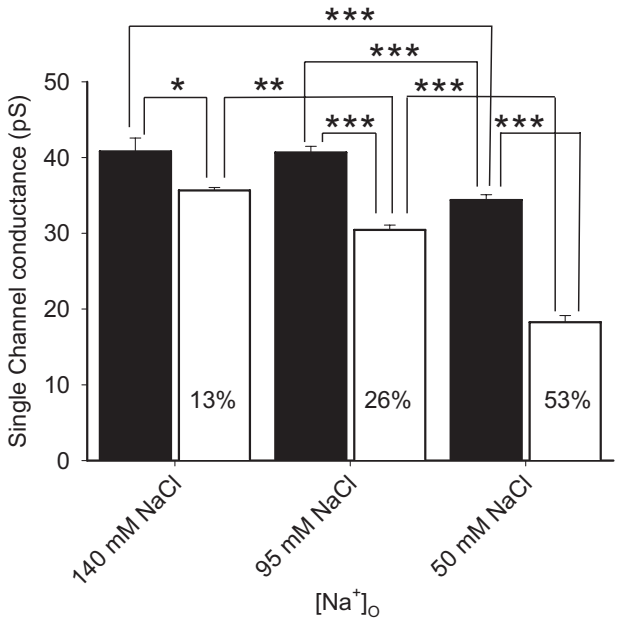

FIGURE 7. **The extracellular concentration of Na^+ influences depression of single channel conductance by extracellular divalent cations.** Bar graph depicting the single channel conductance of the 5-HT_{3A}(QDA) receptor construct in the presence of 0.1 mM Ca^{2+} and 0.1 Mg^{2+} (*black bars*) or 1 mM Ca^{2+} and 2 mM Mg^{2+} (*white bars*) with $[Na^+]_o$ set at 140, 95, or 50 mM. Increasing the extracellular concentration of Ca^{2+} and Mg^{2+} causes a significant reduction of single channel conductance at all concentrations of Na^+ examined, but the magnitude of the depression (expressed as a percentage within the *white bars*) increases as $[Na^+]_o$ is reduced. In the presence of 0.1 mM Ca^{2+} and 0.1 mM Mg^{2+} reducing $[Na^+]_o$ from 140 to 50 mM, but not to 95 mM, significantly decreases single channel conductance. With Ca^{2+} and Mg^{2+} present at 1 and 2 mM, respectively, reducing $[Na^+]_o$ to both 95 and 50 mM causes significant depression of single channel conductance. Data are the mean ± S.E. of observations made from 3–10 outside-out membrane patches. *, $p < 0.05$; **, $p < 0.01$; ***, $p < 0.001$; as determined by analysis of variance followed by Tukey's post hoc test.

Effect of Neutralizing the Extracellular Ring of Charge of the 5-HT_{3A} and 5-HT_{3A}(QDA) Receptor—Extracellular Ca^{2+} exerts multiple effects upon the wild-type 5-HT_{3A} receptor including reductions in the apparent affinity of agonist binding (34, 41), depression of macroscopic and single channel current amplitudes (20, 34, 42), and an acceleration of the kinetics of activation, deactivation, and desensitization (34). Hu and Lovinger (34) demonstrated that neutralization of the extracellular ring of negative charge formed by the 20′ aspartate residue (Fig. 1*B*) at the extracellular vestibule of the mouse 5-HT_{3A} receptor channel by the mutation D298A prevents modulation of macroscopic current kinetics and amplitude by Ca^{2+}. We have examined directly whether the Ca^{2+}-induced decrease in single channel conductance involves the homologous residue (Asp-293) of the human 5-HT_{3A}(QDA) receptor construct and also have evaluated its effect upon the relative permeability to Ca^{2+}. We additionally determined the P_{Ca}/P_{Cs} ratio for 5-HT_{3A} receptors in which the D293A substitution was the only mutation present (*i.e.* 5-HT_{3A}(D293A)).

Application of 1 μM 5-HT to cells transfected with the 5-HT_{3A}(QDA D293A) receptor cDNA elicited only small inward current responses. Hence, we constructed full concentration-response relationships to 5-HT for both the 5-HT_{3A}(QDA) and 5-HT_{3A}(QDA D293A) receptors to determine whether the D293A mutation was associated with a reduction in the agonist potency of 5-HT. Such experiments demonstrated that relative to the 5-HT_{3A}(QDA) receptor ($EC_{50} \approx 1.1$ μM), the 5-HT_{3A}(QDA D293A) construct is less sensitive to 5-HT ($EC_{50} \approx 3.6$ μM; supplemental Fig. 1*A*). Similarly, a comparison of wild-type 5-HT_{3A} and 5-HT_{3A}(D293A) receptors revealed that the D293A mutation decreases the potency of 5-HT, as the EC_{50} value was shifted dextrally from ≈3 to 7 μM (supplemental Fig. 1*B*). In subsequent experiments, 2 μM 5-HT was employed to elicit macroscopic currents from cells expressing the 5-HT_{3A}(D293A) and 5-HT_{3A}(QDA D293A) receptor constructs.

In common with the 5-HT_{3A}(QDA) construct, the 5-HT_{3A}(QDA D293A) mutant maintained exclusive selectivity for cations because the slope of the relationship between the logarithm of $(Na^+)_o$ and $E_{5\text{-HT}}$ was determined to be 61 mV/decade change in $(Na^+)_o$ (Fig. 8*A*). Using solutions E3 and I2 and the voltage ramp protocol, macroscopic currents mediated by the 5-HT_{3A}(QDA D293A) construct in response to 5-HT demonstrated an $E_{5\text{-HT}}$ of −40.5 ± 0.8 mV ($n = 6$), corresponding to a P_{Ca}/P_{Cs} ratio of only 0.25 ± 0.01 ($n = 6$) compared with that of 3.7 for the 5-HT_{3A}(QDA) receptor (Fig. 8*B*). Similarly, the $E_{5\text{-HT}}$ of −30.6 ± 4.7 mV ($n = 6$) for the 5-HT_{3A}(D293A) mutant indicates a P_{Ca}/P_{Cs} of 0.44 ± 0.08 ($n = 6$), which is also significantly reduced *versus* the wild-type receptor (1.4). The P_{Ca}/P_{Cs} ratios of the 5-HT_{3A}(D293A) and 5-HT_{3A}(QDA D293A) receptors were not significantly different. The P_{Na}/P_{Cs} ratio of either construct was unchanged by the D293A mutation (Fig. 8*B*). Thus, for both the wild-type 5-HT_{3A} and 5-HT_{3A}(QDA) constructs, neutralization of the negatively charged 20′ residue greatly reduces the P_{Ca}/P_{Cs} ratio but has no effect upon P_{Na}/P_{Cs}.

In addition to reducing the relative permeability of Ca^{2+}, as evidenced by a decreased sensitivity of $E_{5\text{-HT}}$ to changes in $[Ca^{2+}]_o$ (Fig. 8*C*), the introduction of the D293A mutation into the 5-HT_{3A}(QDA) receptor construct also decreased single channel conductance. In the presence of 0.1 mM Ca^{2+} and 95 mM Na^+, the single channel chord conductance of the 5-HT_{3A}(QDA D293A) receptor was 25.8 ± 1.9 pS ($n = 4$) at a holding potential of −80 mV in comparison with 41.3 pS for the 5-HT_{3A}(QDA) construct. Similarly, the single channel chord conductance (at −80 mV) of the 5-HT_{3A}(QDA D293A) receptor determined with solution E2 (29.8 ± 0.5, $n = 7$) was significantly less than that of the 5-HT_{3A}(QDA) construct (40.8 pS). However, no difference in single channel conductance was observed between the 5-HT_{3A}(QDA) and 5-HT_{3A}(QDA D293A) constructs over a range of positive holding potentials (60 to 100 mV), indicating that the D293A mutation preferentially suppresses inwardly directed cation flux (Fig. 8*D*). As found for the 5-HT_{3A}(QDA) receptor, elevated $[Ca^{2+}]_o$ (0.1–30 mM) also depressed the single channel conductance of the 5-HT_{3A}(QDA D293A) construct in a concentration-dependent manner (Fig. 8*E*). At all values of $[Ca^{2+}]_o$ studied, the single channel chord conductance of the 5-HT_{3A}(QDA D293A) construct was significantly less than that of the 5-HT_{3A}(QDA) receptor. Clearly, the alleviation of macroscopic current block by the D293A mutation (34) cannot be attributed to a reduced influence of Ca^{2+} upon single channel conductance.

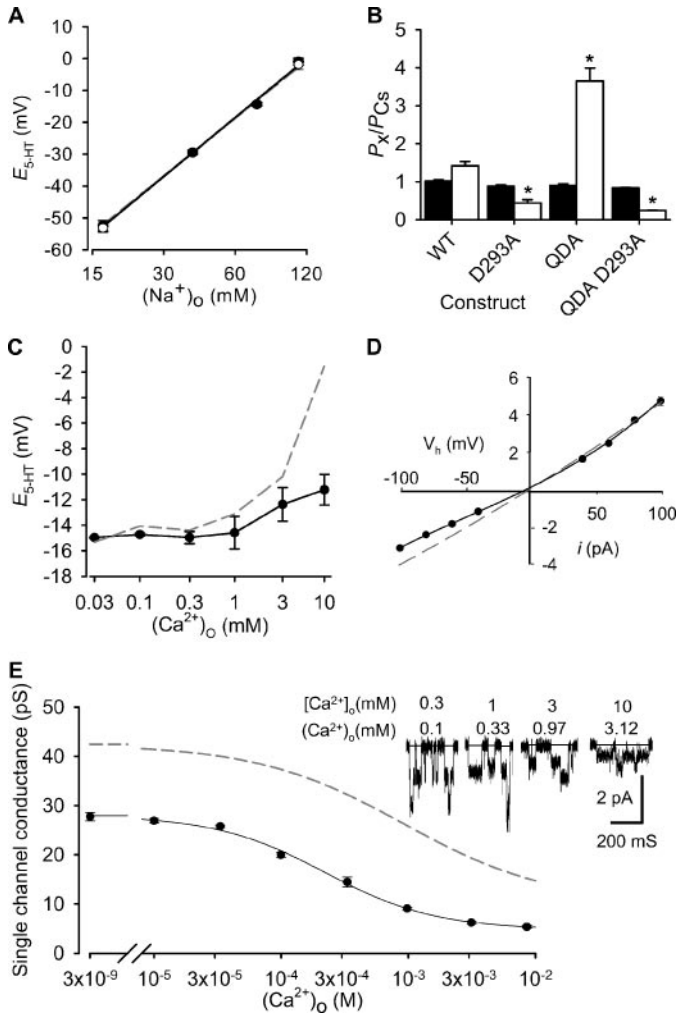

FIGURE 8. **Comparison of the relative ion permeability of wild-type, 5-HT$_{3A}$(D293A), 5-HT$_{3A}$(QDA), and 5-HT$_{3A}$(QDA D293A) receptor constructs with Na^+ and Ca^{2+}.** *A*, the relationship between the reversal potential ($E_{5\text{-HT}}$) of the macroscopic current response to pressure-applied 5-HT (10 μM) recorded from the 5-HT$_{3A}$(QDA D293A) receptor construct and the activity of Na^+ in the extracellular medium ($(Na^+)_o$). Responses were recorded with extracellular electrolytes based on solution E2 wherein the concentration of NaCl was reduced by substitution with sucrose. Intracellular solutions were either CsCl-based I1 (*filled circles*) or a solution in which NaCl totally replaced CsCl (*open circles*). The regression line fitted to the *filled circles* yielded a slope of 61 mV/decade change in $(Na^+)_o$. Data points are the mean of 3–6 independent determinations of $E_{5\text{-HT}}$, and *vertical bars* indicate mean ± S.E. In A, *C*, *D*, and *E*, the *dashed gray lines* summarize the corresponding data for the 5-HT$_{3A}$(QDA) receptor construct illustrated in detail in Figs. 3, 4, and 5. *B*, bar graph illustrating the permeability (P_x/P_{Cs}) of Na^+ (*black bars*) or Ca^{2+} (*white bars*) relative to Cs^+ for the indicated receptor constructs. $E_{5\text{-HT}}$ was determined with an intracellular CsCl-based solution (I1) as reference and NaCl (146 mM)-based solution E2 or with $CaCl_2$ (100 mM)-based solution E3 as the extracellular electrolyte. Data are the mean ± S.E. of 6–17 independent estimates of P_x/P_{Cs}. Mutant constructs in which P_{Ca}/P_{Cs} was significantly different from the wild-type control are indicated with *asterisks* ($p < 0.01$; analysis of variance followed by Dunnett's post hoc test). No significant differences in P_{Na}/P_{Cs} were found between the wild-type and mutant receptors. *C*, $E_{5\text{-HT}}$ for the 5-HT$_{3A}$(QDA D293A) receptor construct with $[Na^+]_o$ set to 95 mM and $[Ca^{2+}]_o$ within the range of 0.1 to 30 mM. Note that Ca^{2+} ion activity ($(Ca^{2+})_o$) rather than concentration ($[Ca^{2+}]_o$) is plotted. Data are the mean of 3–4 observations. *D*, current-voltage (*i-V*) plot for single channel currents recorded from the 5-HT$_{3A}$(QDA D293A) receptor construct with NaCl-based solution E2 as the extracellular electrolyte and I1 as the intracellular solution. Note that the additional D293A mutation causes an intensification of outward rectification and a reduced single channel conductance at negative potentials in comparison with the 5-HT$_{3A}$(QDA) construct. Data are the mean of 6–7 observations. *E*, concentration-response relationship and exemplar single channel currents illustrating the depressant effect of $[Ca^{2+}]_o$ upon the single channel conductance of the 5-HT$_{3A}$(QDA D293A) receptor construct. Note that Ca^{2+} ion activity, rather than concentration, is plotted. Data are the mean ± S.E. of measurements performed on 3–4 outside-out membrane patches at a holding potential of −80 mV under the ionic conditions described in *C*.

DISCUSSION

Two decades of research have focused upon TM2 and flanking sequences as the primary determinants of ion selectivity in Cys-loop receptors (2, 28, 43). For the nicotinic ACh receptor in particular, multiple sites within such domains (*i.e.* the −1′, 13′, 16′, and 17′ positions; Fig. 1*B*) that affect the conduction of Ca^{2+} have been identified (28, 43). We have added to this information by demonstrating that residues within the MA helix of the cytoplasmic loop of the 5-HT$_{3A}$ receptor, a cousin of the nicotinic ACh receptors, exert a strong influence on the permeability of Ca^{2+} relative to monovalent cations. The replacement of arginine residues 432, 436, and 440 of the human 5-HT$_{3A}$ receptor by those aligned in the human 5-HT$_{3B}$ subunit (*i.e.* glutamine, aspartate, and alanine), generating the 5-HT$_{3A}$(QDA) receptor construct, increased P_{Ca}/P_{Cs} from a wild-type value of ~1.4 to 3.7. Such an effect was selective because neither P_{Na}/P_{Cs} nor P_{Na}/P_{Cl} was perturbed by the mutation, the latter being inferred by comparison with values within the literature (20, 29, 30). Notably, the 5-HT$_{3A}$(QDA) construct retained perfect selectivity toward cations *versus* anions, a finding that accords with the results of a recent study in which deletion of the entire intracellular loop of the 5-HT$_{3A}$ receptor had no measurable influence upon P_{Na}/P_{Cl} (44). Indeed, residues within and adjacent to TM2 govern charge selectivity in the 5-HT$_{3A}$ receptor (29). In particular, the single amino acid substitution E−1′A at the intracellular border of TM2 (Fig. 1*B*) is sufficient to generate a 5-HT$_{3A}$ receptor that does not discriminate between monovalent cations and anions ($P_{Na}/P_{Cl} = 0.89$) (30). In future studies, it would be of interest to generate the E−1′A mutation within the 5-HT$_{3A}$(QDA) background to assess whether a role for the MA helix emerges when a primary determinant of charge selectivity is silenced.

Our results indicate that the single mutation R436D is sufficient to enhance P_{Ca}/P_{Cs} to an extent comparable with that found for the 5-HT$_{3A}$(QDA) construct. Analysis of several amino acid substitutions involving neutralization, or inversion, of charge at this key locus suggests that an electrostatic repulsive effect contributes to a suppression of P_{Ca}/P_{Cs} in the wild-type receptor. The latter is consistent with the results of modeling studies that place the highly basic (pK_a = 12.48) guanidinium group of Arg-436 within the intracellular permeation pathways (portals) located between adjacent MA-stretch α-helices (26, 32). Because of the small maximal width of the portals (26), interactions between partially hydrated permeating ions and Arg-436 are likely.

Previous studies of Ca^{2+} permeation through homomeric 5-HT$_3$ receptor channels have, because of its very low single channel conductance, been restricted to the analysis of macroscopic currents. The latter are suppressed by extracellular divalent cations by mechanisms that potentially include a reduction in agonist binding affinity (34, 41), an acceleration of the kinetics of deactivation and desensitization (34), and depression of macroscopic and single channel current amplitudes (20, 34),

the latter being inferred by fluctuation analysis (20). In the present study, we employed the 5-HT_{3A}(QDA) receptor construct to examine directly the influence of extracellular Ca^{2+} upon single channel conductance. A solution (E3), in which Ca^{2+} was the sole extracellular cation, supported outwardly rectifying single channel currents but with a chord conductance at negative potentials (5.7 pS), which was greatly reduced in comparison with the value of 40.8 pS obtained with solution E2, in which Na^+ was the permeant species. Thus, although the permeability of Ca^{2+} relative to Cs^+ is greatly increased in the 5-HT_{3A}(QDA) construct, the channel does not conduct Ca^{2+} efficiently. Moreover, the addition of Ca^{2+} to Na^+-containing extracellular solutions caused a concentration-dependent inhibition of the inwardly directed single channel current amplitude, in a manner reminiscent of that observed for single channel currents mediated by the nicotinic ACh receptor of skeletal muscle (45). Such results are most parsimoniously explained by hypothesizing that the permeation pathway presents a low affinity binding site (or sites) for Ca^{2+}, which confers a degree of selectivity for Ca^{2+} over monovalent cations, yet with an off-rate sufficient to allow significant flux of both Na^+ and Ca^{2+}. An interaction between Ca^{2+} and Na^+ within the channel is supported by our experimental observations indicating the P_{Ca}/P_{Na} ratio for the 5-HT_{3A}(QDA) receptor construct varies with $[Ca^{2+}]_o$ (*i.e.* the principle of independence is violated (39)). Consistent with this notion, the reduction in single channel current amplitude by extracellular divalent cations was more pronounced when $[Na^+]_o$ was reduced.

We considered the D293A residue of the human 5-HT_{3A} receptor subunit, which forms the 20′ negatively charged ring within the extracellular vestibule of the channel (2, 28), to be a strong candidate for the putative Ca^{2+} binding site that limits the rate of charge transfer through the channel (Fig. 1). Firstly, mutation of the corresponding residue (Asp-298) of the mouse 5-HT_{3A} subunit to alanine alleviates the block of macroscopic current responses by extracellular Ca^{2+} (34). Secondly, Ca^{2+} reduced the amplitude of single channel currents mediated by the 5-HT_{3A}(QDA) receptor construct in a voltage-independent manner. The lack of observable voltage dependence suggests a binding site for Ca^{2+} away from the electrical field of the membrane. The 20′ residue resides within such a location. However, because Ca^{2+} is permeant, rather than a simple impermeant open channel blocker, it remains possible that Ca^{2+} does interact with a site(s) within the field but that the increased driving force provided by hyperpolarization facilitates its dissociation and inward conduction. Note that this scenario is quite different from that found for an impermeant cationic blocker, for which the dwell time within the channel would be increased by hyperpolarization because of a decreased probability of the molecule exiting the pore to the extracellular environment.

The potency of 5-HT to activate the mouse 5-HT_{3A}(D298A) construct is less than for the murine wild-type receptor (34), a result concordant with our observation that the D293A mutation introduced into either the human wild-type or 5-HT_{3A}(QDA) construct causes a dextral shift in the 5-HT concentration-response relationship. The D293A mutation within the 5-HT_{3A}(QDA) receptor background caused a reduction in the amplitude of inwardly, but not outwardly, directed single channel current events. Such an effect is consistent with a simple electrostatic mechanism in which the negative charge of the five Asp-293 residues acts to increase the local concentration of permeant cations within the extracellular vestibule. Removal of such charges would thus reduce a focusing mechanism, consistent with the appearance of a enhanced outward rectification in the *i-V* relationship for the 5-HT_{3A}(QDA D293A) receptor construct *versus* the 5-HT_{3A}(QDA) receptor. Very similar effects of neutralizing the extracellular ring of charge upon single channel conductance and rectification have been reported for nicotinic ACh and anion-selective γ-aminobutyric acid type A and glycine receptors (28). Because of the very low conductance of the wild-type 5-HT_{3A} receptor (20, 21) and kinetic properties of the 5-HT_{3A}(D293A) receptor, which are unfavorable to fluctuation analysis (34),[5] we could not estimate the effect of the D293A mutation upon single channel conductance in this construct. However, it is notable that the pattern of inward rectification of macroscopic currents mediated by the mouse 5-HT_{3A}(D298A) mutant resembles that of the murine wild-type receptor (34). The latter differs from the present observations comparing the human 5-HT_{3A}(QDA) and 5-HT_{3A}(QDA D293A) receptors at the single channel level. An important difference in our studies is the removal of positive electrostatic potential in the intracellular vestibule by the mutations R432Q, R436A, and R440A. Such charges are present in the mouse 5-HT_{3A} and 5-HT_{3A}(D298A) receptors studied by Hu and Lovinger (34) and would reduce the local concentration of permeant ions within the intracellular vestibule. The latter would induce a degree of inward rectification. It is possible that such an influence is dominant, masking any tendency toward linearization that might be anticipated from the 5-HT_{3A}(D293A) mutation. Indeed, in our studies, the macroscopic current *I-V* relationship shifts from the pattern of inward rectification characteristic of the wild-type 5-HT_{3A} receptor toward linearity in the 5-HT_{3A}(QDA) construct.

For both the wild-type 5-HT_{3A} and the 5-HT_{3A}(QDA) constructs, the introduction of the D293A mutation drastically reduced the P_{Ca}/P_{Cs} ratio. Once more, such an effect can probably be attributed to a reduction in a local negative electrostatic potential that particularly favors the accumulation of Ca^{2+} at the entrance to the pore, as suggested by molecular dynamics simulations performed on models of the α_7 and skeletal muscle nicotinic ACh receptors (46, 47). Such simulations indicate monovalent cations to be stabilized at the 20′ position, where the ion dwells during its passage through the channel axis. The greater coulombic attraction between Ca^{2+} and the 20′ residue would amplify such interactions. Also, heteromeric $\alpha_4\beta_2$ nicotinic ACh receptors, harboring a larger complement of β_2 subunits in which lysine occupies the 20′ position, appear to have reduced selectivity toward Ca^{2+} (48). However, the D293A residue does not contribute crucially to cation *versus* anion selectivity because the P_{Na}/P_{Cl} ratio for the 5-HT_{3A}(QDA D293A) construct was best described as infinite. A previous study of mouse 5-HT_{3A} receptors in which cysteine residues engineered into the TM2 domain were successfully probed

[5] M. R. Livesey, M. A. Cooper, T. Z. Deeb, J. E. Carland, J. Kozuska, T. G. Hales, J. J. Lambert, and J. A. Peters, unpublished observations.

with a negatively charged sulfydryl-modifying agent (methanethiosulfonate ethylsulfonate (MTSES)) applied extracellularly also indicates that the extracellular ring does not totally select against anions gaining access to deeper regions of the pore (49). In addition, neutralization of the 20′ charge was not required to invert the ion selectivity of the mouse 5-HT_{3A} receptor (29). Finally, the recent crystal structure of a prokaryotic pentameric ligand-gated channel from *Erwinia chrysanthemi* reveals that phenylalanine occupies the 20′ position, yet the channel is cation-selective (50).

Heteromeric 5-HT_3 receptors expressed in tsA-201 cells assemble with the stoichiometry $(5\text{-}HT_{3A})_2(5\text{-}HT_{3B})_3$ as a subunit rosette in the order B-B-A-B-A, yielding 2 × A-B, 2 × B-A, and 1 × B-B subunit interfaces (16). Hence, compared with homomeric receptors, the influence of Arg-432, Arg-436, and Arg-440 will be removed from three of the cytoplasmic portals, irrespective of whether a clockwise or anticlockwise arrangement is assumed. Yet, the inclusion of the 5-HT_{3B} subunit within heteromeric 5-HT_3 receptors reduces permeability to Ca^{2+} (P_{Ca}/P_{Cs} = 0.5–0.6) in comparison with homomeric receptors (P_{Ca}/P_{Cs} = 1.1–1.4) (Ref. 11 and present work). This apparent paradox might be explained by the presence of a polar asparagine, rather than an acidic aspartate, at the 20′ locus and a non-polar alanine, rather than an acidic glutamate, at the −1′ position of the human 5-HT_{3B} *versus* 5-HT_{3A} subunit (Fig. 1*B*). The present work suggests that the 5-HT_{3B} subunit 20′ asparagine may not be optimal for a high P_{Ca}/P_{Cs}, ratio and it is known that a E−1′A substitution in the α_7 nicotinic ACh receptor abolishes permeabilty to Ca^{2+} (28).

Macroscopic current responses mediated by the mouse 5-HT_{3A}(D298A) receptor are insensitive to $[Ca^{2+}]_o$ within the range of 0.1 to 10 mM (34), but we observed that single channel currents recorded from the human 5-HT_{3A}(QDA D293A) receptor were reduced in amplitude in the presence of extracellular Ca^{2+}. Such an effect was concentration-dependent and occurred within the range observed for the 5-HT_{3A}(QDA) receptor. Hence, the Asp-293 residue cannot be a crucial site at which Ca^{2+} binds to reduce single channel conductance in the 5-HT_{3A}(QDA) receptor construct. It remains to be explained why increasing $[Ca^{2+}]_o$ does not affect the macroscopic current response of the mouse 5-HT_{3A}(D298A) receptor, yet clearly depresses single channel conductance in the human 5-HT_{3A}(QDA D293A) construct. However, as clearly noted by Hu and Lovinger (34), depression of single channel conductance cannot be the sole mechanism by which Ca^{2+} depresses macroscopic currents, because the magnitude of the effect is dependent upon the concentration of 5-HT employed to activate the receptor. Indeed, at saturating concentrations of 5-HT (*i.e.* 30 μM), increasing $[Ca^{2+}]_o$ from 1.8 to 10 mM exerts only a modest depressant effect upon 5-HT-evoked currents (34), which might indicate that the influence of Ca^{2+} derives, at least in part, via indirect, or direct, actions upon ligand binding (41). In addition, Ca^{2+} accelerates desensitization of the murine wild-type 5-HT_{3A} receptor, and the D293A mutation suppresses this effect. It is possible that the reduced relative permeability of the 5-HT_{3A}(D293A) mutant contributes to such resistance.

In summary, we have demonstrated that structural elements in both the intracellular and extracellular regions of the human 5-HT_{3A} control relative permeability to Ca^{2+}. Our report represents the first description of the influence of the MA helix upon ion selectivity, a process that has conventionally been linked to specific amino acid residues within TM2 and immediate flanking sequences (28). It is thus an oversimplification to refer to a single selectivity filter in the 5-HT_{3A} receptor and, by inference, in other Cys-loop receptors. Instead, the extracellular vestibule, TM2, and the MA helix act collectively to determine ion permeation.

Acknowledgment—We thank Dr. E. Sher, Eli Lilly and Co., Lilly Research Centre, Windlesham, Surrey, United Kingdom, for support.

REFERENCES

1. Alexander, S. P. H., Mathie, A., and Peters, J. A. (2008) *Br. J. Pharmacol.* **153,** Suppl. 2, S1–S207
2. Peters, J. A., Hales, T. G., and Lambert, J. J. (2005) *Trends Pharmacol. Sci.* **26,** 587–594
3. Thompson, A. J., and Lummis, S. C. R. (2006) *Curr. Pharm. Des.* **12,** 3615–3630
4. Sugita, S., Shen, K. Z., and North, R. A. (1992) *Neuron* **8,** 199–203
5. Roerig, B., Nelson, D. A., and Katz, L. C. (1997) *J. Neurosci.* **17,** 8353–8362
6. Zhou, F. M., and Hablitz, J. J. (1999) *J. Neurophysiol.* **82,** 2989–2999
7. Férézou, I., Cauli, B., Hill, E. L., Rossier, J., Hamel, E., and Lambolez, B. (2002) *J. Neurosci.* **22,** 7389–7397
8. Chameau, P., and van Hooft, J. A. (2006) *Cell Tissue Res.* **326,** 573–581
9. Fink, K. B., and Göthert, M. (2007) *Pharmacol. Rev.* **59,** 360–417
10. Maricq, A. V., Peterson, A. S., Brake, A. J., Myers, R. M., and Julius, D. (1991) *Science* **254,** 432–437
11. Davies, P. A., Pistis, M., Hanna, M. C., Peters, J. A., Lambert, J. J., Hales, T. G., and Kirkness, E. F. (1999) *Nature* **397,** 359–363
12. Dubin, A. E., Huvar, R., D-Andrea, M. R., Pyati, J., Zhu, J. Y., Joy, K. C., Galindo, J. E., Glass, C. A., Luo, L., Jackson, M. R., Lovenberg, T. W., and Erlander, M. G. (1999) *J. Biol. Chem.* **274,** 30799–30810
13. Niesler, B., Frank, B., Kapeller, J., and Rappold, G. A. (2003) *Gene* **310,** 101–111
14. Niesler, B., Walstab, J., Combrink, S., Möller, D., Kapeller, J., Rietdorf, J., Bönisch, H., Gothert, M., Rappold, G., and Brüss, M. (2007) *Mol. Pharmacol.* **72,** 8–17
15. Karnovsky, A. M., Gotow, L. F., McKinley, D. D., Piechan, J. L., Mills, C. J., Schellin, K. A., Slightom, J. L., Fitzgerald, L. R., Benjamin, C. W., and Roberds, S. L. (2003) *Gene* **319,** 137–148
16. Barrera, N. P., Herbert, P., Henderson, R. M., Martin, I. L., and Edwardson, J. M. (2005) *Proc. Natl. Acad. Sci. U. S. A.* **102,** 12595–12600
17. Boyd, G. W., Low, P., Dunlop, J. I., Robertson, L. A., Vardy, A., Lambert, J. J., Peters, J. A., and Connolly, C. N. (2002) *Mol. Cell. Neurosci.* **21,** 38–50
18. Hu, X. Q., and Peoples, R. W. (2008) *J. Biol. Chem.* **283,** 6826–6831
19. Solt, K., Stevens, R. J., Davies, P. A., and Raines, D. E. (2005) *J. Pharmacol. Exp. Ther.* **315,** 771–776
20. Brown, A. M., Hope, A. G., Lambert, J. J., and Peters, J. A. (1998) *J. Physiol.* **507,** 653–665
21. Mochizuki, S., Miyake, A., and Furuichi, K. (1999) *Amino Acids* **17,** 243–255
22. Hales, T. G., Dunlop, J. I., Deeb, T. Z., Carland, J. E., Kelley, S. P., Lambert, J. J., and Peters, J. A. (2006) *J. Biol. Chem.* **281,** 8062–8071
23. Krzywkowski, K., Davies, P. A., Feinberg-Zadek, P. L., Bräuner-Osborne, H., and Jensen, A. A. (2008) *Proc. Natl. Acad. Sci. U. S. A.* **105,** 722–727
24. Brüss, M., Barann, M., Hayer-Zillgen, M., Eucker, T., Göthert, M., and Bönisch, H. (2000) *Naunyn-Schmiedeberg's Arch. Pharmacol.* **362,** 392–401
25. Krzywkowski, K., Jensen, A. A., Connolly, C. N., and Bräuner-Osborne, H. (2007) *Pharmacogenet. Genomics* **17,** 255–266
26. Unwin, N. (2005) *J. Mol. Biol.* **346,** 967–989
27. Sine, S. M., and Engel, A. G. (2006) *Nature* **440,** 448–455

28. Keramidas, A., Moorhouse, A. J., Schofield, P. R., and Barry, P. H. (2004) *Prog. Biophys. Mol. Biol.* **86,** 161–204
29. Gunthorpe, M. J., and Lummis, S. C. R. (2001) *J. Biol. Chem.* **276,** 10977–10983
30. Thompson, A., and Lummis, S. C. R. (2003) *Br. J. Pharmacol.* **140,** 359–365
31. Kelley, S. P., Dunlop, J. I., Kirkness, E. F., Lambert, J. J., and Peters, J. A. (2003) *Nature* **424,** 321–324
32. Deeb, T. Z., Carland, J. E., Cooper, M. A., Livesey, M. R., Lambert, J. J., Peters, J. A., and Hales, T. G. (2007) *J. Biol. Chem.* **282,** 6172–6182
33. Reeves, D. C., Jansen, M., Bali, M., Lemster, T., and Akabas, M. H. (2005) *J. Neurosci.* **25,** 9358–9366
34. Hu, X. Q., and Lovinger, D. M. (2005) *J. Physiol.* **568,** 381–396
35. Fenwick, E. M., Marty, A., and Neher, E. (1982) *J. Physiol.* **331,** 577–597
36. Butler, J. N. (1968) *Biophys. J.* **8,** 1426–1433
37. Wang, J., Liu, W., Fan, J., and Lu, J. (1994) *J. Chem. Soc. Faraday Trans.* **90,** 3281–3285
38. Lewis, C. A. (1979) *J. Physiol.* **286,** 417–445
39. Hille, B. (2001) *Ion Channels of Excitable Membranes*, 3rd Ed., Sinauer Associates, Sunderland, MA
40. Gill, C. H., Peters, J. A., and Lambert, J. J. (1995) *Br. J. Pharmacol.* **114,** 1211–1221
41. Niemeyer, M. I., and Lummis, S. C. R. (2001) *Eur. J. Pharmacol.* **428,** 153–161
42. Hubbard, P. C., and Lummis, S. C. R. (2000) *Eur. J. Pharmacol.* **394,** 189–197
43. Jensen, M. L., Schousboe, A., and Ahring, P. K. (2005) *J. Neurochem.* **92,** 217–225
44. Jansen, M., Bali, M., and Akabas, M. H. (2008) *J. Gen. Physiol.*, **131,** 137–146
45. Dekker, E. R., and Dani, J. A. (1990) *J. Neurosci.* **10,** 3413–3420
46. Ivanov, I., Cheng, X., Sine, S. M., and McCammon, J. A. (2007) *J. Am. Chem. Soc.* **129,** 8217–8224
47. Wang, H.-L., Cheng, X., Taylor, P., McCammon, J. A., and Sine, S. M. (2008) *PloS Comput. Biol.* **4,** e41
48. Tapia, L., Kuryatov, A., and Lindstrom, J. (2007) *Mol. Pharmacol.* **71,** 769–776
49. Panicker, S., Cruz, H., Arrabit, C., and Slesinger, P. A. (2002) *J. Neurosci.* **22,** 1629–1639
50. Hilf, R. J. C., and Dutzler, R. (2008) *Nature* **452,** 375–379
51. Belleli, D., Balcarek, J. M., Hope, A. G., Peters, J. A., Lambert, J. J., and Blackburn, T. P. (1995) *Mol. Pharmacol.* **48,** 1054–1062